Journal of Acupuncture Research

Journal homepage: http://www.e-jar.org

Review Article

A Review of Rat Models of Avascular Necrosis of the Femoral Head Treated with Natural Extracts

Go-Woon Kim [1], Hyoung-Yong Park [2], Yeon-Cheol Park [3,*]

1 Department of Clinical Korean Medicine, Graduate School, Kyung Hee University, Seoul, Korea
2 Department of Science Education, Gyeongin National University of Education, Incheon, Korea
3 Department of Acupuncture and Moxibustion, Kyung Hee University Korean Medicine Hospital, Seoul, Korea

Article history:
Submitted: September 15, 2022
Revised: September 29, 2022
Accepted: October 01, 2022

Keywords:
animal models, avascular necrosis of femoral head, natural extracts, necrosis, osteonecrosis

https://doi.org/10.13045/jar.2022.00227
pISSN 2586-288X eISSN 2586-2898

ABSTRACT

To determine the effect of Korean medicine treatment of avascular necrosis of the femoral head (ANFH) this study reviewed both single ingredients and bioactive compounds in the treatment of ANFH in a rat model. Literature was retrieved from PubMed and Google Scholar using the keywords "femur head necrosis," "natural extract," and "rat." The data from studies analyzed included: rats' characteristics, development methods of ANFH, natural extracts administration, observation methods, and outcome indicators. Two independent researchers screened all articles retrieved and 26 studies were chosen. The most used rat species was the Sprague Dawley rat (76.9%). To induce ANFH, steroid injections (46.2%), and oral gavage (53.8%) were typically used. Studies focused mainly on factors affecting bone formation (65.3%), and apoptosis (53.8%). Research on ANFH focused on using traditional natural substances mentioned in classical literature to confirm its effectiveness against anti-inflammation, osteogenesis, and cell death. ANFH has a diverse etiology, therefore research models such as genetic analysis of human-derived samples from ANFH patients may shed more light on the condition. Moreover, research into herbal medicines and pharmacoacupuncture treatment of ANFH should precede.

Introduction

Avascular necrosis of the femoral head (ANFH) is where necrosis, due to various causes, occurs in the femoral head where there has been disruption to the blood supply [1]. ANFH, an intractable condition/disease, has been increasingly detected in recent years mainly due to the increased use of steroids and improvements in radiological technology.

Despite extensive research, in most cases the clear cause of ANFH cannot be identified owing to various complex factors. Sometimes ANFH may be linked to trauma, alcohol, steroid treatment in patients with autoimmune diseases, and several diseases such as hereditary thrombosis, lupus, hemoglobinopathy, and chronic renal disease [1,2]. The pathology of ANFH currently is as follows: accumulated cell stress, fat emboli, and coagulopathy due to various factors leading to lowered blood flow which can cause ischemia and eventually lead to bone necrosis [2].

Treatment can be categorized into surgical and non-surgical intervention. Surgical treatment is performed according to the characteristics of the lesion, stage, type, patient's age, and occupation. Preservative non-surgical treatment is recommended for younger patients without head collapse [3]. Non-surgical treatments include physiotherapy, weight-bearing restrictions, and medicinal drug treatment (anticoagulants, vasodilators, and

***Corresponding author.** Yeon-Cheol Park
Department of Acupuncture and Moxibustion, Kyung Hee University Korean Medicine Hospital, 892, Dongnam-ro, Gangdong-gu, Seoul, Korea
E-mail: icarus08@khu.ac.kr
ORCID: Go-Woon Kim https://orcid.org/0000-0002-5609-6430, Hyoung-Yong Park https://orcid.org/0000-0002-6358-4635, Yeon-Cheol Park https://orcid.org/0000-0002-8805-9212

phosphates). However, there is no clear evidence that the types of drugs utilized to treat ANFH stop the progress of bone necrosis. Moreover, some drugs have several side effects e.g., osteonecrosis of the mandible with a relatively high proportion of cortical bone and atypical fracture of the femur [3,4].

Clinical research and experimental research studies have reported the efficacy of Korean medicinal treatments such as acupuncture, pharmacoacupuncture, and herbal medicine in treating musculoskeletal diseases [5-8]. In clinical practice, various Korean medicine treatments such as pharmacoacupuncture have been reported to be effective treatments for ANFH [9].

However, to develop a better understanding of the application of Korean medicine treatments for ANFH, we need to identify the components of Korean medicine treatments that contribute to anti-inflammation, pain control, and bone protection which are disease-specific for ANFH. Therefore, this study reviewed rat models of ANFH to assess treatment outcomes using single ingredients and bioactive compounds.

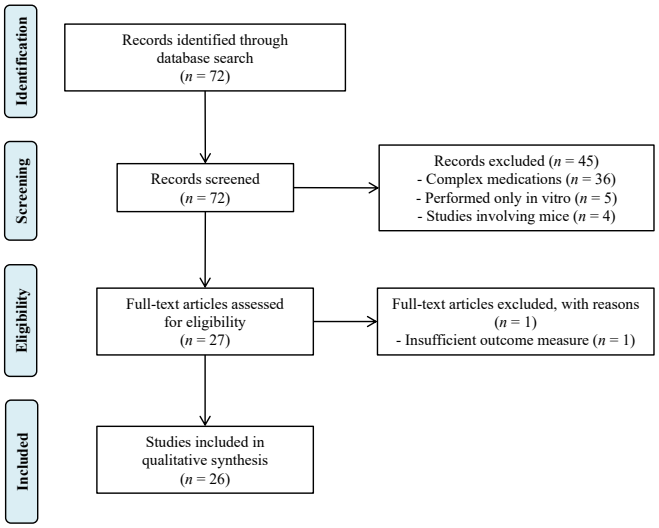

Fig. 1. Flow diagram of the selection of articles.

Materials and Methods

The PubMed database was searched for publications prior to April 26, 2022. The following search string was used: ["Femur Head Necrosis"(Mesh)] AND ["Rats" (Mesh)]. From the 184 results retrieved, research related to natural substances was selected. The Google Scholar database was also searched for publications published before April 26, 2022, up to 99 pages. The search term used was: (Femur Head Necrosis) AND (natural extract) AND (rat). There was no limits on the language.

In this review, the focus was on studies of water- or alcohol-based natural extracts or bioactive compounds of natural substances. In addition to avascular necrosis, general bone necrosis on the femoral head was included. Although in vivo studies of natural extracts were included, studies on complex medications such as herbal medicines, were excluded. In addition, studies involving mice and those performed only in vitro were excluded. Among the selected articles, those that showed insufficient results were excluded.

Data regarding the following parameters were extracted: authors, publication year, animal species, sex, number of animals, induction type/period, administration route/period, morphological observation, anti-inflammatory action, apoptosis, bone formation, angiogenesis, adipogenesis, and safety assessment.

Results

The initial search included 72 articles. After screening titles and abstracts, 45 articles were excluded based on the selection criteria for this study. After a full-text assessment, one more article was excluded. There were 26 articles eligible for review (Fig. 1; Tables 1-3 [10-35]).

Among the rat species used in the studies, Sprague-Dawley (SD) rats (76.9%) were the most commonly used species, followed by Wistar rats (23.1%). Male rats (61.5%) were preferred. The most commonly used method for induction of ANFH was the steroid-only method (46.2%). Among these steroids, dexamethasone (26.9%) was used the most, followed by methylprednisolone acetate (7.7%), prednisolone acetate (7.7%), and methylprednisolone (3.8%). Among the selected articles, eight (30.8%) studies used both endotoxins and steroids. Moreover, all eight articles used lipopolysaccharide (LPS) as the endotoxin, and methylprednisolone (26.9%) was the most commonly used steroid in this combination, though methylprednisolone sodium succinate (3.8%) was also used. In addition, 5 studies used liquid containing alcohol for the induction of ANFH (19.2%), while the surgical method (3.8%) was the least used. Regarding the administration of a single ingredient or bioactive compound, oral gavage and intraperitoneal injection were used in 53.8% and 38.5% of the studies, respectively.

Histological analysis using hematoxylin and eosin (H&E) staining (92.3%) was the predominant stain used for the morphological assessment of ANFH, followed by micro-computed tomography (micro-CT, 42.3%), angiography using micro-CT (11.5%), and dual-energy X-ray absorptiometry (7.7%). The incidence rate (53.8%) and empty lacunae rate (46.2%) were used for histological analysis, which was highly comparable with the determined number of rats with ANFH according to the appraisal standard.

Two studies examined inflammation (7.7%): interleukin (IL)-1 beta (IL-1β), IL-6, and tumor necrosis factor-alpha were measured in both studies, while p65, toll-like receptor 4, and myeloid differentiation primary response 88 were measured in one study (3.8 %).

Factors related to apoptosis were determined in 14 articles (53.8%), with terminal deoxynucleotidyl transferase-mediated dUTP nick-end labeling (38.5%) being the most commonly used method. B-cell lymphoma-2 (bcl-2, 26.9%), bcl-2-associated X (26.9%), caspase-3 (26.9%), caspase-9 (11.5%), and cytochrome c (11.5%) were also studied.

Factors related to bone formation were identified in 17 (65.3 %) articles. Alizarin Red S staining (30.8%) and dynamic bone formation using the fluorochrome labeling assay (15.4%) were used in the aforementioned articles. Osteocalcin (38.5%), alkaline phosphatase (42.3%), runt-related transcription factor 2 (38.5%), collagen Type 1 (26.9%), bone morphogenetic protein 2 (19.2%),

Table 1. Summarized Data from Included Articles (2010–2014).

Material/ authors (y)	Species/ sex (*N*)	Induction type (time/period)	Administration method (period)	Outcome measures						Safety assessment
				Morphological obs.	Inflammation	Apoptosis	Bone formation	Angiogenesis	Adipogenesis	
Cervi Cornu */ Shi et al [10] (2010)	Wistar/ male (*52*)	DEX i.m. inj. (50 mg/kg) (2 times/wk, 6 wk)	OG (60 d)	TEM · Bone cell lesion ↓	N/A	N/A	HOP ↓, HOM ↑ HOM/ HOP ratio ↑ [in vitro] OB cell, ALP activity ↑ Proportion of S phase cell ↑ Proportion of G0/G1 cell ↓	N/A	N/A	SR, CS, BW
Epimedium brevicornum */ Wang et al [11] (2011)	SD m:f = 1:1 (*48*)	PSL acetate i.m. inj. (12.5 mg/kg) (2 times/wk, 4 wk)	OG (20 d)	H&E · Incidence rate ↓	N/A	N/A	OPG ↑, RANKL ↓ OPG/RANKL ratio ↑	N/A	N/A	SR
Cervi Cornu */ Pharhat B et al [12] (2011)	Wistar/ male (*42*)	DEX i.m inj. (30 mg/kg) (2 times/wk, 6 wk)	OG (60 d)	DEXA · BMD ↑ H&E · Tb.Th ↑, Tb.Sp ↓ · Bone cell lesion ↓ · Adipose cell ↓ · Hematopoietic cell ↑	N/A	N/A	N/A	VEGF ↑	TC, LDL ↓ TG ↑	SR, CS, BW
Gastrodin †/ Zheng et al [13] (2014)	Wistar male (*18*)	LPS i.v. inj. (1.8 mg/kg) (2 d) MPS i.m. inj. (25 mg/kg) (5 d)	i.p. (28 d)	H&E · Incidence rate ↓	N/A	TUNEL (+) ↓ Bax, Caspase-3 ↓ Bcl-2 ↑ Bax/Bcl-2 ↓	N/A	N/A	N/A	SR
Achyranthes bidentata */ Jiang et al [14] (2014)	Wistar/ male (*105*)	MPSL s.c. inj. (21 mg/kg) (6 wk)	OG (24 d)	Micro CT · Tb.Th, Tb.Pf, Tb.N, BV/TV, BMD ↑ · Tb.Sp, SMI ↓ Micro CT AG · Hematopoietic cell ↑ H&E · Empty lacunae rate ↓ · Bone cell lesion ↓ · Adipose cell ↓	N/A	N/A	TRAP (+) ↓ BAP activity ↓ OPG ↑ RANK, RANKL ↓ RANKL/OPG ratio ↓ [in vitro] TRAP (+) ↓ OPG ↑ RANKL, RANKL/ OPG ratio ↓	Vessel thickness ↑ Vessel volume ↑ Vessel surface area to vessel volume ↑	TC, TG, LDL ↓ ApoA1, ApoB ↓ HDL ↑	N/A
Cajanus cajan */ Shi et al [15] (2014)	SD/ male (*40*)	Surgery (puncturing)	BMSCs lesion inj. (1 time) cajan leaf lesion inj. (30 d)	H&E · Bone cell lesion ↓ · Adipose cell ↓ · Hematopoietic cell ↑	N/A	N/A	Chondrocytes no. ↑	VEGF ↑	N/A	N/A

* Single ingredient.
† Bioactive compound.
AG, angiography; ALP, alkaline phosphatase; ApoA1, apolipoprotein A1; ApoB, apolipoprotein B; BAP, bone-specific alkaline phosphatase; BMD, bone mineral density; BMSCs, bone marrow mesenchymal stem cells; BV/TV, bone volume/tissue volume; BW, body weight; CS, clinical signs; DEX, dexamethasone; DEXA, Dual-energy X-ray absorptiometry; H&E, hematoxylin and eosin staining; HDL, high-density lipoprotein cholesterol; HOM, hexosamine; HOP, hydroxyproline; i.m., intramuscular; i.p., intraperitoneal; i.v., intravenous; inj., injection; LDL, low-density lipoprotein cholesterol; LPS, lipopolysaccharide; Micro CT, Micro computed tomography; MPS, methylprednisolone; MPSL, methylprednisolone acetate; N/A, not applicable; no., number; OB, osteoblast; obs., observation; OG, oral gavage; OPG, osteoprotegerin; PSL, prednisolone; RANK, receptor activator of nuclear factor kappa B; RANKL, RANK ligand; SD, Sprague-Dawley; SMI, structure model index; SR, survival rate; Tb.N, trabecular number; Tb.Pf, trabecular bone pattern factor; Tb.Sp, trabecular separation; Tb.Th, trabecular thickness; TC, total cholesterol; TEM, Transmission electron microscopy; TG, triglyceride; TRAP, Tartrate-resistant acid phosphatase; TUNEL, TdT mediated dUTP nick-end labelling; VEGF, vascular endothelial growth factor.

Table 2. Summarized Data from Included Articles (2015-2018).

Material/ authors (y)	Species/ sex (*N*)	Induction type (time/period)	Administration method (period)	Outcome measures						Safety assessment
				Morphological obs.	Inflammation	Apoptosis	Bone formation	Angiogenesis	Adipogenesis	
Saponins of panax notoginseng */ Yuan et al [16] (2015)	SD/ male (*30*)	DEX i.m. inj. (50 mg/kg) (2 times/wk, 6 wk)	i.p. (24 d)	H&E · Bone cell lesion ↓ · Adipose cell ↓	N/A	TUNEL (+), Caspase-3 ↓ [In vitro] TUNEL, Hoechst 33258 (+) ↓ Caspase-3 activity ↓	N/A	VEGF-A ↑	N/A	N/A
Tetramethylpyrazine*/ Jiang et al [17] (2015)	Wistar/ male (*85*)	MPSL s.c. inj. (21 mg/kg) (6 wk)	i..m. (24 d)	Micro CT · Tb.Th, Tb.Pf, Tb.N ↑ BV/TV, BMD ↑ · Tb.Sp, SMI ↓ Micro CT AG H&E · Incidence rate ↓ · Empty lacunae rate ↓ · Bone cell lesion ↓ · Adipose cell ↓	N/A	N/A	N/A	Vessel thickness ↑ Vessel volume ↑ Vessel surface area to vessel volume ↑ VEGF, FLK1 ↑	TG, TC, LDL ↓ ApoA1, ApoB ↓ HDL ↑	SR, CS, BW
Muscone */ Guo et al [18] (2017)	SD/ N/A (*30*)	Ethanol-containing Lieber-DeCarli liquid diet (6 wk)	i.p. (24 wk)	Micro CT · BV/TV, BMD ↑ H&E · Incidence rate ↓ MT · Bone cell lesion ↓	N/A	N/A	MT (+) ↑ COL1, OCN ↑ [in vitro] ARS (+) ↑ COL1, OCN, RUNX2 ↑ ALP activity ↑	N/A	N/A	BW
Cordycepin */ Chen et al [19] (2017)	SD/ N/A (*30*)	Ethanol-containing Lieber-DeCarli liquid diet (6 wk)	i.p. (24 d)	Micro CT · BV/TV, Tb.Th ↑ H&E · Incidence rate ↓	N/A	TUNEL (+) ↓	COL1, OCN ↑ [in vitro] ALP activity, COL1, OCN ↑ BMP2, RUNX2, β-catenin ↑	N/A	N/A	BW, CS
Epimedium brevicornum */ Liu et al [20] (2018)	SD/ m:f = 1:1 (*24*)	PSL acetate i.m. inj. (15 mg/kg) (2 times/wk, 6 wk)	OG (24 d)	H&E · Empty lacunae rate ↓ BMD ↑	N/A	Bcl-2 ↑ LC3-II, Beclin1 ↓ LC3-II/LC3I ↓	N/A	N/A	N/A	N/A
Icariin */ Huang et al [21] (2018)	SD/ female (*30*)	LPS i.v. inj. (10 μg/kg) (2 d) MPS i.m. inj. (20 mg/kg) (3 d)	OG (48 d)	Micro CT · BMD, BV/TV, BS/TV ↑ Tb.N, Tb.Th ↑, Tb.Sp ↓ H&E · Incidence rate ↓ · Bone cell lesion ↓ · Adipose cell ↓	N/A	N/A	RUNX2, ALP ↑ [in vitro] ARS (+) ↑ ALP activity ↑ ALP, BMP2, OCN, RUNX2 ↑	N/A	ORO (+) ↓ TG, PPARγ ↓ [In vitro] ORO (+) ↓ TG, PPARγ ↓	N/A
Salidroside */ Xue et al [22] (2018)	SD/ male (*45*)	LPS i.p. inj. (40 μg/kg) (2 d) MPSS i.m. inj. (40 mg/kg) (3 d)	i.p (7 d)	H&E · Empty lacunae rate ↓ · Incidence rate ↓	N/A	[In vitro] Bcl-2 ↑ Caspase-3,9 ↓ Cyt c, Bax ↓	N/A	N/A	N/A	N/A

* Single ingredient.
† Bioactive compound.
AG, angiography; ALP, alkaline phosphatase; ApoA1, apolipoprotein A1; ApoB, apolipoprotein B; ARS, Alizarin Red S staining; BMD, bone mineral density; BMP2, bone morphogenetic protein 2; BS/TV, bone surface/total volume; BV/TV, bone volume/tissue volume; BW, body weight; COL1, collagen type I; CS, clinical signs; cyt c, cytochrome c; DEX, dexamethasone; FLK1, fetal liver kinase 1; H&E, hematoxylin and eosin staining; HDL, high-density lipoprotein cholesterol; i.m., intramuscular; i.p., intraperitoneal; i.v., intravenous; inj., injection; LC3, microtubule-associated protein 1 light chain 3; LDL, low-density lipoprotein cholesterol; LPS, lipopolysaccharide; Micro CT, Micro computed tomography; MPS, methylprednisolone; MPSL, methylprednisolone acetate; MPSS, methylprednisolone sodium succinate; MT, Masson's Trichrome Staining; N/A, not applicable; obs., observation; OCN, osteocalcin; OG, oral gavage; ORO, oil red O staining; PPARγ, peroxisome proliferator-activated receptor gamma; PSL, prednisolone; RUNX2, Runt related transcription factor 2; SD, Sprague-Dawley; SMI, structure model index; SR, survival rate; Tb.N, trabecular number; Tb.Pf, trabecular bone pattern factor; Tb.Sp, trabecular separation; Tb.Th, trabecular thickness; TC, total cholesterol; TG, triglyceride; TUNEL, TdT mediated dUTP nick-end labelling; VEGF, vascular endothelial growth factor.

Table 3. Summarized Data from Included Articles (2019–2022).

Material/ authors (y)	Species/ sex (*N*)	Induction type (time/period)	Administration method (period)	Outcome measures						Safety assessment
				Morphological obs.	Inflammation	Apoptosis	Bone formation	Angiogenesis	Adipogenesis	
Icariin†/ Yu et al [23] (2019)	SD/ N/A (*30*)	LPS i.p. inj. (10 μg/kg) (2 d) MPS i.m. inj. (40 mg/kg) (3 times/d, 3 d)	OG (24 d)	Micro CT AG H&E · Incidence rate ↓ · Empty lacunae rate ↓	N/A	[In vitro] Bax ↓ Bcl-2 ↑	[in vitro] BMECs migration ↑ Wound recovery ↑	Vessel volume ↑ CD31 ↑ [in vitro] Tube length ↑ Branch no. ↑ VEGF, CD31, vWF ↑	N/A	SR
Safflower†/ Cui et al [24] (2019)	Wistar/ male (*40*)	DEX i.m. inj. (50 mg/kg) (2 times/wk, 6 wk)	OG (60 d)	DEXA · BMD ↑ H&E · Empty lacunae rate ↓ · Bone cell lesion ↓ · Adipose cell ↓	N/A	TUNEL (+) ↓	HOP ↓, HOM ↑ HOM/HOP ratio ↑	N/A	N/A	N/A
Ginsenoside Rb1†/ Ye et al [25] (2019)	SD/ male (*30*)	DEX i.m. inj. (50 mg/kg) (2 times/wk, 6 wk)	OG (21 d)	H&E · Bone cell lesion ↓	IL1β , IL6, TNFα, p65 ↓	Bax ↓ Caspase-3, p53 ↓	BMP2, RUNX2, OCN ↑ ALP, OCN activity ↑	VEGF, VEGFR ↑	TC, LDL/HDL ↓ MDA ↓ SOD, CAT ↑ GSHPX ↑	N/A
Betaine†/ Yang et al [26] (2019)	SD/ male (*30*)	Ethanol-containing drinking water (6 wk)	i.p. (6 wk)	Micro CT · BMD, BV/TV ↑ Tb.Th, Tb.N ↑ · Incidence rate ↓ Fluorochrome labeling · MAR ↑ H&E · Bone cell lesion ↓	N/A	TUNEL (+) ↓	Dynamic bone formation area ↑ OCN, COL1 ↑ [in vitro] ARS (+) ↑ ALP activity ↑ BMP2, OCN, RUNX2 ↑	N/A	N/A	BW
Chrysophanic acid†/ Yu et al [27] (2020)	SD/ male (*30*)	Ethanol-containing Lieber-DeCarli liquid diet (6 wk)	i.p. (24 d)	Micro CT · BMD, BV/TV ↑ Tb.Th, Tb.N ↑ Fluorochrome labeling H&E · Incidence rate ↓ · Bone cell lesion ↓	N/A	TUNEL (+) ↓	COLI, OCN ↑ Dynamic bone formation area ↑ [In vitro] ARS, ALP (+) ↑ COL1, OCN, OPN, RUNX2, PI3K ↑	N/A	[In vitro] ORO (+) ↓ Leptin, PPARγ ↓ LPL ↓	BW, CS, SR
Crocin†/ Li et al [28] (2020)	SD/ m:f = 1:1 (*30*)	LPS i.v. inj. (10 μg/kg) (1 time) MPS i.m. inj. (20 mg/kg) (3 times/d, 5 d)	OG (14 d)	H&E · Empty lacunae rate ↓ · Bone cell lesion ↓	N/A	N/A	COL1A1, OCN, RUNX2 ↑ GSK-3β ↓ [in vitro] ARS (+), ALP activity ↑ COL1A1, OCN, RUNX2 ↑ GSK-3β ↓	N/A	N/A	N/A
Osthole†/ Yu et al [29] (2020)	SD/ male (*30*)	Ethanol-containing Lieber-DeCarli liquid diet (6 wk)	i.p. (24 d)	Micro CT · BMD, BV/TV ↑ Tb.N, Tb.Th ↑ Fluorochrome labeling H&E · Incidence rate ↓	N/A	TUNEL (+) ↓	COLI, OCN ↑ Dynamic bone formation area ↑ [in vitro] ARS (+) ↑ ALP activity ↑ COLI, OCN, OPN, RUNX2, β-catenin ↑	[in vitro] Branch point no. ↑ tube formation ↑ VEGF ↑	[In vitro] ORO (+) ↓ Leptin, PPARγ ↓	N/A

Table 3. (continued).

Material/ authors (y)	Species/ sex (*N*)	Induction type (time/period)	Administration method (period)	Outcome measures						Safety assessment
				Morphological obs.	Inflammation	Apoptosis	Bone formation	Angiogenesis	Adipogenesis	
Luteolin†/ Yan et al [30] (2020)	SD/ N/A (*30*)	DEX i.m. inj. (10 mg/kg) (2 times/wk, 8 wk)	OG (32 d)	Micro CT · BMD, BV/TV, Tb.N ↑ Tb.Sp ↓ H&E · Incidence rate ↓ · Empty lacunae rate ↓	N/A	Caspase-3 ↓ [In vitro] TUNEL (+) ↓ Bcl-2 ↑ Caspase-3,9 ↓ Cyt c, Bax ↓	N/A	N/A	N/A	N/A
Allicin†/ Zhan et al [31] (2020)	SD/ male (*45*)	DEX i.m. inj. (10 mg/kg) (2 times/wk, 8 wk)	OG (32 d)	Micro CT · BMD, BV/TV ↑ Tb.N, Tb.Th ↑, Tb.Sp ↓ H&E · Incidence rate ↓ · Empty lacunae rate ↓	N/A	Caspase-3 ↓ [In vitro] TUNEL (+) ↓ Bcl-2 ↑ Caspase-3,9 ↓ Cyt c, Bax ↓	N/A	N/A	N/A	N/A
Calycosin†/ Zhu et al [32] (2021)	SD/ male (*60*)	MPS i.m. inj. (30 mg/kg) (3 days/wk, 3 wk)	i.p. (21 d)	Micro CT · BMD, BV/TV ↑ Tb.N, Tb.Th ↑, Tb.Sp ↓ Microfil perfusion H&E · Incidence rate ↓ · Bone cell lesion ↓	TNF-α, TLR4 ↓ Myd88 ↓ IL-1β, IL-6 ↓ [In vitro] TNF-α, TLR4, Myd88 ↓ IL-1β, IL-6 ↓	N/A	BMP2, COL1, OCN ↑ Dynamic bone formation area ↑ [in vitro] ARS (+) ↑ ALP activity ↑ BMP2, COL1, OCN ↑	Vessel volume ↑ Microvessel density ↑	N/A	N/A
Icariin†/ Yue et al [33] (2021)	SD/ female (*90*)	LPS i.p. inj. (20 μg/kg) (2 d) MPS i.m. inj. (40 mg/kg) (3 d)	OG (24 d)	Microscope obs. · Empty lacunae rate ↓ · Bone cell lesion ↓ · Hematopoietic cell ↑	N/A	N/A	N/A	TM, VEGF ↓ Lumen no. ↑ [in vitro] miRNA-335 ↓ Living cells ↑ Scratch closure rate ↑ (cell migration)	N/A	N/A
Total flavonoids of Rhizoma drynariae†/ Lv et al [34] (2021)	SD/ male (*24*)	LPS i.m. inj. (40 μg/kg) (2 d) MPS i.m. inj. (40 mg/kg) (3 d)	i.p. (5 d)	H&E · Empty lacunae rate ↓	N/A	TUNEL (+) ↓ Bax, Caspase-3 ↓ Bcl-2 ↑ ROS production ↓ [In vitro] Bax, Caspase-3 ↓ Bcl-2 ↑ Apoptotic rate ↓	OCN, OPG, RUNX2 ↑ RANKL ↓	VEGF ↑	N/A	SR, BW
Lycium barbarum polysaccharide†/ Song et al [35] (2022)	SD/ N/A (*NA*)	LPS i.p. inj. (20 μg/kg) (2 d) MPS i.m. inj. (40 mg/kg) (3 d)	OG (4 wk)	H&E · Empty lacunae rate ↓ · Bone cell lesion ↓	N/A	N/A	ARS (+) ↑ [in vitro] ARS (+) ↑ RUNX2, ALP ↑ Annexin V/PI (+) ↓	N/A	N/A	BW, BG

* Single ingredient.
† Bioactive compound.
AG, angiography; ALP, alkaline phosphatase; ARS, Alizarin Red S staining; BG, blood glucose; BMD, bone mineral density; BMP2, bone morphogenetic protein 2; BMSCs, bone marrow mesenchymal stem cells; BV/TV, bone volume/ tissue volume; BW, body weight; CAT, chloramphenicol acetyltransferase; CD31, cluster of differentiation 31; COL1, collagen type I; COL1A1, collagen type I alpha1; CS, clinical signs; cyt c, cytochrome c; DEX, dexamethasone; DEXA, Dual-energy X-ray absorptiometry; GSK-3β, glycogen synthase kinase-3β; H&E, hematoxylin and eosin staining; HDL, high-density lipoprotein cholesterol; HOM, hexosamine; HOP, hydroxyproline; i.m., intramuscular; i.p., intraperitoneal; i.v., intravenous; IL, Interleukin; inj., injection; LDL, low-density lipoprotein cholesterol; LPL, lipoprotein lipase; LPS, lipopolysaccharide; MAR, mineral apposition rate; MDA, malondialdehyde; Micro CT, Micro computed tomography; MPS, methylprednisolone; MT, Masson's Trichrome Staining; N/A, not applicable; no., number; obs., observation; OCN, osteocalcin; OG, oral gavage; OPG, osteoprotegerin; OPN, osteopontin; ORO, oil red O staining; PI, propidium iodide; PI3K, phosphoinositide 3-kinase; PPARγ, peroxisome proliferator-activated receptor gamma; RANKL, receptor activator of nuclear factor kappa B ligand; ROS, reactive oxygen species; RUNX2, Runt related transcription factor 2; SD, Sprague-Dawley; SOD, superoxide dismutase; SR, survival rate; Tb.N, trabecular number; Tb.Sp, trabecular separation; Tb.Th, trabecular thickness; TC, total cholesterol; TLR4, tolllike receptor 4; TM, thrombomodulin; TNF, tumor necrosis factor; TUNEL, TdT mediated dUTP nick-end labelling; VEGF, vascular endothelial growth factor; VEGFR, VEGF receptor; vWF, von Willebrand factor.

osteoprotegerin (11.5%), and receptor activator of nuclear factor kappa B ligand (11.5%) were also identified.

Angiogenesis was assessed in 11 articles (42.3%) and angiography using micro-CT (11.5%), and microfilm perfusion (3.8%) were used as the methods. Vascular endothelial growth factor (VEGF, 34.6%) was mainly observed factor.

Factors related to adipogenesis were identified in seven articles (26.9%), in which Oil Red O staining (11.5%) was used. Total cholesterol (15.4%), triglycerides (15.4%), low-density lipoprotein cholesterol (LDL, 15.4%), high-density lipoprotein cholesterol (11.5%), and peroxisome proliferator-activated receptor gamma (PPARγ, 11.5%) levels were measured.

Of all the selected articles, six (23.1%) studies used water- or alcohol-based extraction of single ingredient natural substances , and 20 studies used the bioactive compounds derived from natural substances, including epimedium and icariin (5 cases, 19.2%), antler (2 cases, 7.7%), Rhizoma drynariae and luteolin (2 cases, 7.7%). Twelve articles (46.2%) mentioned the stability of each single ingredient and bioactive compound, and six articles (23.1%) reported that the single ingredient or bioactive compounds used in the study alleviated symptoms of ANFH in a dose-dependent manner.

Discussion

Rats are commonly used animals in research for many reasons; they grow fast, are easy to handle, and share physiological and metabolic traits with humans [36]. Furthermore, ANFH induced rats clearly display the early stages of ANFH clinical pathology, which are difficult to study in humans [37]. However, rats differ in many aspects depending on the species. For instance, SD rats originate from the selective breeding of Wistar rats [38]. SD rats have different bone characteristics than Wistar rats for example SD rats have a much faster rate of progression of osteoporosis and show more dramatic articular atrophy [39]. For these reasons, SD rats are the most commonly used animals in research. Huang et al [21] and Yue et al [33] studied the estrogen-like activities of icariin in female rats. However, except for gender-specific research, male SD rats are normally used.

There were four methods used to induce ANFH: steroid treatment, steroids with LPS injection, oral administration of ethanol, and surgery. The use of steroids induces histological evidence of the early stages of ANFH [40]. It has been reported by Zhan et al [31] that inducing ANFH with dexamethasone alone takes a long time but has the benefit of having a mechanism similar to that in humans. The incidence rate of ANFH depends on the type, volume, and frequency of steroid administration [36]. Among the studies where steroid-induced ANFH was performed and the incidence rate was reported, subcutaneous injection of methylprednisolone acetate (21 mg/kg) for 6 weeks showed the highest rate of induction of ANFH, Jiang et al [17] reported a 92% rate of induction. Moreover, steroid induction is related to adipogenesis, apoptosis of osteocytes and osteoblast, fat embolism, vascular thrombosis, and oxidative stress [41]. Thus, steroid-only induction is suitable for studies on effect an ingredient or compound has on a particular mechanism.

In the studies included in this review, apoptosis, bone formation, and angiogenesis were reported to be the most common mechanisms in steroid-only induced ANFH studies, and adipogenesis was also observed four times. All studies that confirmed inflammation used steroid-only induced ANFH [25,32].

LPS, also known as an endotoxin, is used along with steroids to induce inflammation [36]. Using a LPS with steroids results in a shorter induction time, a larger area of bone necrosis, and a higher death rate compared with single steroid induction of ANFH [40]. In the studies reviewed, the average induction period for the use of a single steroid was 5.9 weeks. On the other hand, using LPS with steroids took an average of 5.38 days to induce ANFH. Induction of ANFH with LPS and steroids has been reported to result in a relatively high death rate [40]; however, no study in this review has reported death using LPS with steroids.

Inflammation induced by LPS hinders vascular function, induces apoptosis of osteoblasts, suppresses bone formation, increases bone resorption, and downregulates osteocalcin expression [42]. The use of LPS with steroids is a suitable method for studying materials that have these mechanisms. In this review, studies using LPS with steroids for induction of ANFH have mostly confirmed bone formation and apoptosis.

Rat models of ANFH using ethanol are useful for investigating the cause of disease associated with alcohol and evaluating treatment [40].

It has been reported that 4-6 months of oral gavage administration of over 45% ethanol in rats can induce bone necrosis, but 7 days of administration of 5% ethanol can also induce bone necrosis [43]. The Lieber-DeCarli liquid diet is commonly used for ethanol induction and has the advantage of efficient use of ethanol in animal experiments [43,44]. Among the articles in this review, studies using the Lieber-DeCarli liquid diet used 8% ethanol. Only the study by Yang et al [26] used 5% to 30% ethanol, increasing by 5% every week, but the reason for this was not stated.

Inducing ANFH using ethanol can cause hyperlipidemia. However, it has been reported that this has no relation to proinflammatory reactions via toll-like receptor 4, which plays an important role in alcoholic fatty liver disease [43]. All five studies that used ethanol to induce ANFH studied bone formation-related mechanisms, and apoptosis was studied in four of the articles. Two studies examined the mechanisms of adipogenesis. Research performed by Yu et al [27] proposed that adipogenesis induced by ethanol is related to the AMPK pathway, and that it can be alleviated by chrysophanic acid.

Chemical induction and non-traumatic drug models of ANFH result in a vast area of the femoral head being necrotized, thus have the disadvantage of not being able to precisely imitate the clinical situation [45]. However, surgery-induced necrosis is closely related to blood circulation damage near the femoral head and has the advantage of reflecting the pathology of traumatic ANFH [40].

In this review, only one study by Shi et al [15], used surgery for the induction of ANFH. The vast majority of studies focused only on ANFH induced by steroids or ethanol, this may be a result of the expertise required to perform surgical methods to induce ANFH. The traditional method of inducing ANFH by surgery involves cutting all retinacular blood vessels and the round ligament of the

femoral head to induce femoral head dislocation. However, a new model of trauma induced ANFH has been reported whereby partial blood vessel abrasion of the femoral head is performed to interrupt the blood supply [45].

Comparing the 14 studies in this review that reported the incidence rate, the five studies that used steroids only reported an average incidence rate of 81.02%, four studies using steroids with LPS reported an average incidence rate of 79.99%, and four studies using ethanol induction of ANFH reported an average incidence rate of 78%. Therefore, average incidence rate between these methods of inducing ANFH was similar.

Steroid-only induction of ANFH is a suitable model for studying anti-inflammatory and adipogenesis-related mechanisms. It has also been associated with apoptosis, bone formation, and angiogenesis. Steroids with LPS for the induction of ANFH can be used to answer questions concerning anti-inflammatory mechanisms, apoptosis, and bone formation quickly. Ethanol induction of ANFH can be used to observe apoptosis, bone formation, and adipogenesis which may give insight into alcohol induced ANFH caused in patients who are alcoholics. For research on traumatic ANFH, induction surgery is the most suitable method of inducing ANFH.

Rat models of steroid induction of ANFH under hypoxic conditions [46], surgical induction of ANFH considering ageing and bone repair [47], and ANFH induction caused by tobacco smoke [48] have been reported since 2020. By using the appropriate rat model for the induction of ANFH which suits the disease characteristics (mechanism, purpose of study, and bone condition) of interest, the relevant mechanisms of action can be studied in the future.

Single ingredients and bioactive compounds were administered orally, intraperitoneally, intramuscularly, and locally. Different organs and pathways are responsible for the metabolism of each drug; thus, different effects may appear depending on the method of administration. The administration route must always be considered so that an unsuitable administration method is not used [49,50]. Differences in the methods of drug administration were not reviewed in this study.

Following 3-8 weeks post ANFH induction (average 5.7 weeks) the rats were sacrificed but no reason was given in any of the 7 studies for the choice of time point [13,17,22,28,31,32,34].

For morphological observations of induced ANFH micro-CT and angiography, sample observation, dual-energy X-ray absorptiometry, and histological analysis were used. Micro-CT is preferred by many researchers owing to its short scan time and non-invasive features. Furthermore, geometric analysis using morphological parameters, visualized using micro-CT, such as bone mineral density, bone volume, and trabecular thickness, are highly related to actual bone strength data that can be obtained using mechanical tests [51,52]. MRI is superior to normal radiographs because abnormalities in the bone interface can be observed [53]. Use of MRI as a very sensitive method for the early diagnosis of induced ANFH is advisable.

The rate of empty lacunae, which is the main characteristic of osteonecrosis in histological observations, and the incidence rate (according to histological diagnosis criteria) were measured and evaluated in several studies. Empty lacunae not only showed the degree of osteonecrosis but were also used as an index to compare between studies [54].

Staining with H&E was mainly used for microscopic observation, and bone cell lesions were observed using various histological characteristics such as the number, volume, density, and arrangement of trabeculae, as well as the degree of bone marrow cell debris accumulation. Three studies directly observed a sample of femoral head, and it was confirmed that the ANFH-induced femoral head showed cyanosis [30,31] and brittleness [23].

Toxicity was assessed using change in weight, survival rate, clinical signs, and blood glucose. The survival rate was mainly used to assess toxicity, but only Wang et al [11] reported deaths during the study period. Clinical signs such as activity and behavioral changes, physical appearance (e.g., fluffy hair), and joint exudate were observed [10,12,17,19,27]. It has been reported that toxicity can be assessed more precisely by observing clinical signs such as weight loss (of over 5%), piloerection, half-shut eyes, and motor activity [55].

Factors such as the levels of IL-1β, IL-6, and tumor necrosis factor-alpha have been studied in relation to inflammation, and bcl-2 and bcl-2-associated X have been studied with respect to apoptosis. Typical osteogenic factors, such as collagen Type 1 and osteocalcin, were studied as the factors most related to the osteogenic mechanism, while VEGF and PPARγ were observed to assess angiogenesis and adipogenesis, respectively. The most important signaling pathways in the pathological development of ANFH are osteogenesis-related phosphatidylinositol 3-kinase/protein kinase B signaling, receptor activator of nuclear factor kappa B ligand/receptor activator of nuclear factor kappa B/osteoprotegerin signaling, Wnt/β-catenin pathway, apoptosis-related Wnt/β-catenin, STAT1/caspase3, angiogenesis-related VEGF/FLK1 signaling, and lipogenesis-related PPARγ-mediated signaling pathways. However, the anti-inflammatory cytokines, t helper 17 (Th17) cells and IL-17 [56], and the apoptotic reactive oxygen species/c-Jun N-terminal kinases/c-Jun pathways [57] are recent areas of interest; thus, these mechanisms should be further elucidated in future studies.

Only bioactive compounds were studied after 2015, with the exception of the study by Liu et al [20]. Half of the studies on single ingredients were extracted using water, and there have been no studies on the differential effects of extraction methods. Of the single ingredients and bioactive compounds, Epimedium brevicornum was the most studied, and Cervi Cornu and R. drynariae were studied twice each. Traditional Korean medicine texts state that E. brevicornum displays properties relating to "strengthening sinews and bones" and "warming the kidney and invigorating yang." Thus, E. brevicornum is widely used to treat knee and back pain, and as a tonic for aphrodisiacs, improving bone strength, and kidney health [11,21,23]. E. brevicornum is also commonly used to treat ANFH and osteoporosis [11,23]. Moreover, through pharmacological studies, E. brevicornum has been reported to have anti-inflammatory, anti-osteoporosis, blood circulation-improving, and anti-aging effects, and is also involved in the phosphatidylinositol 3-kinase/protein kinase B and epidermal growth factor/epidermal growth factor receptor signaling

pathways [11,20,21,23,33].

The research articles on induced ANFH included in this review were varied. Of the many proposed mechanisms of ANFH, apoptosis, inflammation, lipid metabolism disorders, insufficient blood supply, and osteogenic/osteoclastic differentiation were the main focuses. In recent studies, Th17 cells and synovial cells in synovial tissue and the interactions between these cells have received much attention as key mechanisms, however, more research is necessary. Discovering a clinically effective treatment is difficult. ANFH is an intractable joint disease that interacts with various pathological mechanisms.

Conclusion

It is necessary to develop a rat model suitable to study the pathophysiology of ANFH. Specifically, to understand the action of immunomodulatory mechanisms and pathways such as those influenced by Th17 cells and their production of IL-17. In addition, it is essential to study the materials that affect Korean medicine pattern identification which is similar to the pathophysiology of ANFH (e.g., essence and blood deficiency, and dampness-heat). Furthermore, research limitations involved in single mechanisms need to be overcome by establishing the basis for diagnosis and treatment using Korean medicine by using next-generation sequencing analysis of tissue samples from ANFH patients.

Author Contributions

Conceptualization: GWK and YCP. Methodology: HYP and YCP. Formal investigation: GWK and YCP. Data analysis: GWK and YCP. Writing original draft: GWK. Writing - review and editing: HYP and YCP.

Conflicts of Interest

The authors have no conflicts of interest to declare.

Funding

None.

Ethical Statement

This research did not involve any human or animal experiments.

Data Availability

All relevant data are included in this manuscript.

References

[1] Zalavras CG, Lieberman JR. Osteonecrosis of the Femoral Head: Evaluation and Treatment. J Am Acad Orthop Surg 2014;22:455-464.
[2] Guerado E, Caso E. The physiopathology of avascular necrosis of the femoral head: An update. Injury 2016;47:S16-S26.
[3] Joint Surgery Group of the Orthopaedic Branch of the Chinese Medical Association. Guideline for Diagnostic and Treatment of Osteonecrosis of the Femoral Head: Guideline for Osteonecrosis Femoral Head. Orthop Surg 2015;7:200-207.
[4] Lim YW, Kim YS, Kwon SY. Joint Preserving Non-surgical Treatment of Osteonecrosis of Femoral Head. J Korean Hip Soc 2012;24:273-278. [in Korean].
[5] Jia M, Nie Y, Cao DP, Xue YY, Wang JS, Zhao L et al. Potential Antiosteoporotic Agents from Plants: A Comprehensive Review. Evid Based Complement Alternat Med 2012;2012:364604.
[6] Tang H, Hosein A, Mattioli-Belmonte M. Traditional Chinese Medicine and orthopedic biomaterials: Host of opportunities from herbal extracts. Mater Sci Eng C Mater Biol Appl 2021;120:111760.
[7] Kim KH, Kim TH, Lee BR, Kim JK, Son DW, Lee SW et al. Acupuncture for lumbar spinal stenosis: a systematic review and meta-analysis. Complement Ther Med 2013;21:535-556.
[8] Lee YJ, Jo HR, Kim SH, Sung WS, Kim EJ. Efficacy and Safety of Pharmacopuncture and Bee Venom Acupuncture for Knee Osteoarthritis: A Systematic Review and Meta-Analysis. J Korean Med 2020;41:55-83. [in Korean].
[9] Kim DH, Kim EJ, Jo MJ. Two Case Reports of Patients Diagnosed with Avascular Necrosis of the Femoral Head Treated with Korean Medicine Treatment Including Chuna Manual Therapy, Pharmacopuncture and Acupuncture. J Korean Med Rehabil 2021;31:195-204. [in Korean].
[10] Shi B, Li G, Wang P, Yin W, Sun G, Wu Q et al. Effect of antler extract on corticosteroid-induced avascular necrosis of the femoral head in rats. J Ethnopharmacol 2010;127:124-129.
[11] Wang JZ, Gao HY, Wang KZ, Zhou RX, Li XD, Guo J et al. Effect of Epimedium extract on osteoprotegerin and RANKL mRNA expressions in glucocorticoid-induced femoral head necrosis in rats. Nan Fang Yi Ke Da Xue Xue Bao 2011;31:1714-1717. [in Chinese].
[12] Pharhat B, Peng H, Li B, Huang L. Effects of antler powder on treatment of corticosteroidinduced avascular necrosis of the femoral head in rats. Chin J Tissue Eng Res 2011;15:4541-4544.
[13] Zheng H, Yang E, Peng H, Li J, Chen S, Zhou J et al. Gastrodin prevents steroid-induced osteonecrosis of the femoral head in rats by anti-apoptosis. Chin Med J (Engl) 2014;127:3926-3931.
[14] Jiang Y, Zhang Y, Chen W, Liu C, Li X, Sun D et al. Achyranthes bidentata extract exerts osteoprotective effects on steroid-induced osteonecrosis of the femoral head in rats by regulating RANKL/RANK/OPG signaling. J Transl Med 2014;12:334.
[15] Shi D, Sun Y, Yin J, Fan X, Duan H, Liu N et al. Cajan leaf combined with bone marrow-derived mesenchymal stem cells for the treatment of osteonecrosis of the femoral head. Exp Ther Med 2014;7:1471-1475.
[16] Yuan HF, Pan JF, Li S, Guo CA, Liu SH, Yan ZQ. Protective Effects of Total Saponins of Panax Notoginseng on Steroid-Induced Avascular Necrosis of the Femoral Head In Vivo and In Vitro. Evid Based Complement Alternat Med 2015;2015:165679.
[17] Jiang Y, Liu C, Chen W, Wang H, Wang C, Lin N. Tetramethylpyrazine Enhances Vascularization and Prevents Osteonecrosis in Steroid-Treated Rats. BioMed Res Int 2015;2015:315850.
[18] Guo YJ, Luo SH, Tang MJ, Zhou ZB, Yin JH, Gao YS et al. Muscone exerts protective roles on alcohol-induced osteonecrosis of the femoral head. Biomed Pharmacother 2018;97:825-832.
[19] Chen YX, Zhu DY, Xu ZL, Yin JH, Yu XW, Mei J et al. The Protective Effect of Cordycepin On Alcohol-Induced Osteonecrosis of the Femoral Head. Cell Physiol Biochem 2017;42:2391-2403.
[20] Liu S, Huang Y, Wang C, Tian S, Xu Y, Ge J. Epimedium protects steroid-induced avascular necrosis of femoral head in rats by inhibiting autophagy. Exp Ther Med 2018;16:5047-5052.
[21] Huang Z, Cheng C, Cao B, Wang J, Wei H, Liu X et al. Icariin Protects against Glucocorticoid-Induced Osteonecrosis of the Femoral Head in Rats. Cell Physiol Biochem 2018;47:694-706.
[22] Xue X, Feng Z, Li Z, Pan X. Salidroside inhibits steroid-induced avascular necrosis of the femoral head via the PI3K/Akt signaling pathway: In vitro and in vivo studies. Mol Med Rep 2018;17:3751-3757.
[23] Yu H, Yue J, Wang W, Liu P, Zuo W, Guo W et al. Icariin promotes

angiogenesis in glucocorticoid-induced osteonecrosis of femoral heads: In vitro and in vivo studies. J Cell Mol Med 2019;23:7320-7330.
[24] Cui D, Zhao D, Huang S. Beneficial contribution of a safflower (Carthamus tinctorius L.) polysaccharide on steroid-induced avascular necrosis of the femoral head in rats. Int J Biol Macromol 2019;123:581-586.
[25] Ye J, Wei D, Peng L, Chang T. Ginsenoside Rb1 prevents steroid-induced avascular necrosis of the femoral head through the bone morphogenetic protein-2 and vascular endothelial growth factor pathway. Mol Med Rep 2019;20:3175-3181.
[26] Yang Q, Yin W, Chen Y, Zhu D, Yin J, Zhang C et al. Betaine alleviates alcohol-induced osteonecrosis of the femoral head via mTOR signaling pathway regulation. Biomed Pharmacother 2019;120:109486.
[27] Yu H, Liu P, Zhu D, Yin J, Yang Q, Huang Y et al. Chrysophanic acid shifts the differentiation tendency of BMSCs to prevent alcohol-induced osteonecrosis of the femoral head. Cell Prolif 2020;53:e12871.
[28] Li B, Qin K, Wang B, Liu B, Yu W, Li Z et al. Crocin promotes osteogenesis differentiation of bone marrow mesenchymal stem cells. Vitro Cell Dev Biol Anim 2020;56:680-688.
[29] Yu H, Zhu D, Liu P, Yang Q, Gao J, Huang Y et al. Osthole stimulates bone formation, drives vascularization and retards adipogenesis to alleviate alcohol-induced osteonecrosis of the femoral head. J Cell Mol Med 2020;24:4439-4451.
[30] Yan Z, Zhan J, Qi W, Lin J, Huang Y, Xue X et al. The Protective Effect of Luteolin in Glucocorticoid-Induced Osteonecrosis of the Femoral Head. Front Pharmacol 2020;11:1195.
[31] Zhan J, Yan Z, Zhao M, Qi W, Lin J, Lin Z et al. Allicin inhibits osteoblast apoptosis and steroid-induced necrosis of femoral head progression by activating the PI3K/AKT pathway. Food Funct 2020;11:7830-7841.
[32] Zhu D, Yu H, Liu P, Yang Q, Chen Y, Luo P et al. Calycosin modulates inflammation via suppressing TLR4/NF-κB pathway and promotes bone formation to ameliorate glucocorticoid-induced osteonecrosis of the femoral head in rat. Phytother Res 2021;35:2824-2835.
[33] Yue J, Yu H, Liu P, Wen P, Zhang H, Guo W et al. Preliminary study of icariin indicating prevention of steroid-induced osteonecrosis of femoral head by regulating abnormal expression of miRNA-335 and protecting the functions of bone microvascular endothelial cells in rats. Gene 2021;766:145128.
[34] Lv W, Yu M, Yang Q, Kong P, Yan B. Total flavonoids of Rhizoma drynariae ameliorate steroid-induced avascular necrosis of the femoral head via the PI3K/AKT pathway. Mol Med Rep 2021;23:345.
[35] Song Q, Yong HM, Yang LL, Liang YQ, Liu ZX, Niu DS et al. Lycium barbarum polysaccharide protects against osteonecrosis of femoral head via regulating Runx2 expression. Injury 2022;53:1361-1367.
[36] Xu J, Gong H, Lu S, Deasey MJ, Cui Q. Animal models of steroid-induced osteonecrosis of the femoral head - a comprehensive research review up to 2018. Int Orthop 2018;42:1729-1737.
[37] Kerachian MA, Harvey EJ, Cournoyer D, Chow TY, Nahal A, Séguin C. A rat model of early stage osteonecrosis induced by glucocorticoids. J Orthop Surg Res 2011;6:62.
[38] Himmler SM, Modlinska K, Stryjek R, Himmler BT, Pisula W, Pellis SM. Domestication and diversification: A comparative analysis of the play fighting of the Brown Norway, Sprague-Dawley, and Wistar laboratory strains of (Rattus norvegicus). J Comp Psychol 2014;128:318-327.
[39] Warmink K, Rios JL, van Valkengoed DR, Korthagen NM, Weinans H. Sprague Dawley Rats Show More Severe Bone Loss, Osteophytosis and Inflammation Compared to Wistar Han Rats in a High-Fat, High-Sucrose Diet Model of Joint Damage. Int J Mol Sci 2022;23:3725.
[40] Fan M, Peng J, Qin L, Lu S. Experimental animal models of osteonecrosis. Rheumatol Int 2011;31:983-994.
[41] Weinstein RS. Glucocorticoid-Induced Bone Disease. N Engl J Med 2011;365:62-70.
[42] Zheng LZ, Wang JL, Kong L, Huang L, Tian L, Pang QQ et al. Steroid-associated osteonecrosis animal model in rats. J Orthop Translat 2018;13:13-24.
[43] Okazaki S, Nagoya S, Tateda K, Katada R, Mizuo K, Watanabe S et al. Experimental rat model for alcohol-induced osteonecrosis of the femoral head. Int J Exp Pathol 2013;94:312-319.
[44] Lieber CS, DeCarli LM, Sorrell MF. Experimental methods of ethanol administration. Hepatology 1989;10:501-510.
[45] Lv Y, Qiu X, Liu G, Wang Y, Zhang Y, Li W et al. A novel model of traumatic femoral head necrosis in rats developed by microsurgical technique. BMC Musculoskelet Disord 2022;23:374.
[46] Yin BH, Chen HC, Zhang W, Li TZ, Gao QM, Liu JW. Effects of hypoxia environment on osteonecrosis of the femoral head in Sprague-Dawley rats. J Bone Miner Metab 2020;38:780-793.
[47] Yamaguchi R, Kamiya N, Kuroyanagi G, Ren Y, Kim HKW. Development of a murine model of ischemic osteonecrosis to study the effects of aging on bone repair. J Orthop Res 2021;39:2663-2670.
[48] Xu J, Qiu X, Yu G, Ly M, Yang J, Silva RM et al. Soluble epoxide hydrolase inhibitor can protect the femoral head against tobacco smoke exposure-induced osteonecrosis in spontaneously hypertensive rats. Toxicology 2022;465:153045.
[49] Chen MM, Palmer JL, Ippolito JA, Curtis BJ, Choudhry MA, Kovacs EJ. Intoxication by Intraperitoneal Injection or Oral Gavage Equally Potentiates Postburn Organ Damage and Inflammation. Mediators Inflamm 2013;2013:971481.
[50] Hu SC, Bryant MS, Sepehr E, Kang HK, Trbojevich R, Lagaud G et al. Toxicokinetic and Genotoxicity Study of NNK in Male Sprague Dawley Rats Following Nose-Only Inhalation Exposure, Intraperitoneal Injection, and Oral Gavage. Toxicol Sci 2021;182:10-28.
[51] Bagi CM, Hanson N, Andresen C, Pero R, Lariviere R, Turner CH et al. The use of micro-CT to evaluate cortical bone geometry and strength in nude rats: Correlation with mechanical testing, pQCT and DXA. Bone 2006;38:136-144.
[52] Hildebrand T, Laib A, Müller R, Dequeker J, Rüegsegger P. Direct Three-Dimensional Morphometric Analysis of Human Cancellous Bone: Microstructural Data from Spine, Femur, Iliac Crest, and Calcaneus. J Bone Miner Res 1999;14:1167-1174.
[53] Chen XC, Weng J, Chen XQ, Du JZ, Zhu MP, Pan YQ et al. Relationships among magnetic resonance imaging, histological findings, and IGF-I in steroid-induced osteonecrosis of the femoral head in rabbits. J Zhejiang Univ Sci B 2008;9:739-746.
[54] Xie XH, Wang XL, Yang HL, Zhao DW, Qin L. Steroid-associated osteonecrosis: Epidemiology, pathophysiology, animal model, prevention, and potential treatments (an overview). J Orthop Transl 2015;3:58-70.
[55] Silva AV. Associations between clinical signs and pathological findings in toxicity testing. ALTEX 2021;38:198-214.
[56] Zou D, Zhang K, Yang Y, Ren Y, Zhang L, Xiao X et al. Th17 and IL-17 exhibit higher levels in osteonecrosis of the femoral head and have a positive correlation with severity of pain. Endokrynol Pol 2018;69:283-290.
[57] Peng P, Nie Z, Sun F, Peng H. Glucocorticoids induce femoral head necrosis in rats through the ROS/JNK/c-Jun pathway. FEBS Open Bio 2021;11:312-321.